

Calldown Frequencies from Circular Orbits to a Specified Landing Site

F. MARTIKAN*

General Precision, Inc., Binghamton, N. Y.

Introduction

THE performance of a recoverable space vehicle can be measured by the number and distribution of times the vehicle can be recalled and landed at a specified site. A general method to determine calldown frequency is necessary for answers to design considerations, such as optimization of orbital parameters for a large recall capability with a short waiting time in orbit or determination of the sensitivity of calldown frequency to individual trajectory parameters. Calldown frequency estimates are useful for preliminary orbit design for recoverable boost vehicles, transports from manned or unmanned space stations, orbital data drops, descent from parking orbits for lunar and interplanetary missions, and more sophisticated space missions that have a near-earth orbital phase.

The ascent, orbital, and descent phases all affect the calldown frequency. Although numerous papers have discussed these three phases individually, very few considered the entire trajectory from launch to landing. Rosamond¹ considers the touchdown accuracy of retrorocket-recovered satellites with nonlifting re-entry vehicles and minimizes the effects of burn-out errors by proper selection of the deorbit thrust. His results were obtained from numerical integrations of the equations of motion. Jensen et al.² present an analysis of calldown frequency, but their method is accurate only for polar orbits or arbitrarily inclined orbits without lateral maneuverability and they use an arbitrary tolerance of ± 0.01 orbital revolution to increase rather than reduce the calldown frequency. Some of these restrictions and some typographical errors are corrected in a later publication.³

In the present paper, results from the three trajectory phases are combined in a method to determine recall times from circular orbits of any orbital altitude and inclination to a specified site. The concept of a ground swath is introduced to account more accurately for lateral maneuverability; arbitrarily shaped descent envelopes can be approximated. An average computing time (IBM 7094) for one calldown frequency table for a two-week orbital mission is about 2 sec.

Mathematical Model

The ascent trajectory is considered to determine the initial point in orbit for a specified launch site and booster. Small errors in the injection point do not affect calldown materially; they merely shift the succeeding trajectory. However, secular effects on the orbit plane location and on the period while the vehicle is in orbit may become significant because of their cumulative effect on future vehicle positions over a rotating earth. Thus adherence to a nominal calldown schedule reduces to period control and a loose tolerance on the inclination.

The space vehicle is represented by a mass point in a circular orbit with a given inclination i , $0^\circ \leq i \leq 180^\circ$ and mean initial orbital radius r_i . The altitude h of the circular orbit is defined as its mean equatorial altitude $h = r - R_e$ where r is

the mean geocentric radius and R_e the equatorial radius of the earth. Secular oblateness and atmospheric drag effects are superimposed on the earth's central force field, but periodic oblateness effects, gravitational attractions of other celestial bodies, solar radiation pressure, and mass irregularities of the earth are assumed to be negligible. The main effect of atmospheric drag is to decrease the mean orbital radius and the period. The radius of the j th revolution r_j is given in terms of quantities of the $(j-1)$ th revolution:

$$r_j = r_{j-1} - 4\pi B_{\text{eff}} \rho_{j-1} r_{j-1}^2 \quad (1)$$

where

$$B_{\text{eff}} = F_{ao}(\rho_{\text{dispersed}}/\rho_{\text{std atm}})C_D A/2M$$

is the effective ballistic coefficient, $F_{ao}(h, i)$ the atmospheric oblateness correction factor,⁴ C_D the drag coefficient, A the frontal area of the space vehicle, M its mass, and ρ the atmospheric density computed from the 1962 U. S. Standard Atmosphere.⁵ The factor $(\rho_{\text{dispersed}}/\rho_{\text{std atm}})$ is introduced to enable simulation of constant dispersions in atmospheric density from the standard. The change in period of the j th revolution corresponding to the decrease in radius is

$$\Delta\tau_j = -(12\pi^2/\mu^{0.5})B_{\text{eff}}\rho_{j-1}r_{j-1}^{2.5} \quad (2)$$

where $\mu = GM_e$ is the gravitational constant of the earth. Secular effects of earth oblateness are summarized by the nodal regression rate,

$$\dot{\Omega} = -3\pi J_2 (R_e/r_i)^2 \cos i \text{ [rad/rev]} \quad (3)$$

where $J_2 \simeq 1082.61 \times 10^{-6}$ is the second zonal harmonic coefficient in the expansion of the earth's gravitational potential, and a correction to the nodal period of the space vehicle,

$$\Delta\tau_{ob} = -\frac{3\pi}{\mu^{0.5}} r_i^{1.5} J_2 \left(\frac{R_e}{r_i}\right)^2 \frac{7 \cos^2 i - 1}{4} \quad (4)$$

(Both expressions have been discussed by the author and Kalil.⁶) Very small orbital eccentricities are simulated by introducing a correction $\Delta\tau_d$ to the period for k revolutions, at which time a circularizing maneuver to r_k is assumed to take place. This simplified correction is valid for the present mathematical model only as long as the differences of drag and oblateness effects on the circular and very low-eccentricity orbit are of second order.

Calldown is possible only when the landing site, which is on the rotating earth, is within the maneuvering envelope. Define a maneuvering envelope as the boundary of points on earth which can be reached from an instantaneous orbital position by either aerodynamic maneuvering or modification of the deorbit thrust vector. This envelope is assumed independent of i and orbital central angle ϕ , whereas any altitude dependence is considered by introducing several envelopes for the expected deorbit altitude ranges. A point inside the envelope is defined on a nonrotating earth by a longitudinal range in the orbit plane R_d from deorbit, and a lateral range R_{lat} , with lateral ranges in the direction of the space vehicle angular velocity considered positive. For computing convenience, each irregular maneuvering envelope is approximated by one or more "maneuvering rectangles" on the spherical earth. Two "corners" of this rectangle are defined by $(R_d)_{\text{min}}$, the corresponding $(t_d)_{\text{min}}$, and $(R_{\text{lat}})_{\text{max}}$ as well as $(R_{\text{lat}})_{\text{min}}$, respectively. Similarly, the other two corners are given by $(R_d)_{\text{max}}$, $(t_d)_{\text{max}}$, $(R_{\text{lat}})_{\text{max}}$, and $(R_{\text{lat}})_{\text{min}}$. This definition is possible since t_d is only very weakly dependent on R_{lat} . Measures of landing site "nearness" to the orbital plane are $(R_{\text{lat}})_{\text{max}}$ and $(R_{\text{lat}})_{\text{min}}$, which form a ground swath around the space vehicle ground track. For calldown to be possible, the geocentric parallel of latitude of the landing site θ , must intersect or lie wholly within the ground swath. The permissible range of ϕ from which deorbit with a subsequent landing at the specified site is possible depends on both

Received December 5, 1963; revision received September 10, 1964. This work was performed while the author was with the Martin Company, Baltimore, Md. The author wishes to thank L. Sternfield, Manager of the Martin Company Aerospace Mechanics Department, for permission to publish this paper and H. Coley and B. Stech, Digital Computing Section, for their skillful programing. Appreciation is also due F. Kalil and G. Townsend for comments and discussions.

* Staff Engineer, Systems Engineering Department, Link Group. Member AIAA.

longitudinal and lateral maneuverability. The relative importance of either depends on i and θ_f .

The mathematical model for elliptic orbits would be more complex, because the secular variations in the semimajor axis, eccentricity due to atmospheric drag, and the precession of the perigee due to oblateness would have to be included in analytical form for the orbital phase, and the variation of the maneuvering envelope with ϕ would have to be taken into account.

Calldown Conditions

Two algebraic equations and three constraints are used to determine calldown. The first equation is obtained by considering the total displacement in longitude and the time from launch to landing and then solving for the number of orbital revolutions n . Unfortunately, n occurs also in the upper limit of a summation in the same equation, so that one can solve for it only approximately. The second equation is obtained by considering the total ϕ from injection to deorbit, and it contains n and p , the integer number of orbital revolutions. The three constraints are on the longitude λ_f of the landing site, the range of ϕ required for landing, and R_d . Calldown is possible if, with the lower and upper limits of the constraints satisfied, the equations can be satisfied simultaneously.

Illustrative Example

Consider a typical 10-day space station mission. The vehicle is initially at an altitude of 150 naut miles at its ascending node on the Greenwich meridian. For an assumed on-orbit ballistic coefficient $B = C_{DA}/2M = 0.25 \text{ ft}^2/\text{slug}$, the altitude loss due to drag during the 10 days is about 4.6 naut miles. It is required to determine the effect of lateral maneuverability on the subsequent calldown frequency to a landing site in central Texas ($\theta_f = 30^\circ \text{ N}$, $\lambda_f = 100^\circ \text{ W}$). For simplicity, six maneuvering rectangles have been considered. The smallest rectangle is defined by $R_{lat} = \pm 150$ naut miles and $R_d = \pm 250$ naut miles from the nominal descent range. The larger rectangles are increased by a constant ratio from this one. The effect of rectangle size on t_d has been neglected.

Calldown characteristics can be presented in tabular form by showing whether it can or cannot take place on a given orbital revolution. However, when a relatively long time period is considered, it is more illuminating to give the number of calldowns separately from the maximum delay time, i.e., the longest time between successive calldowns, as we do here in Figs. 1 and 2.

The results can be easily interpreted by use of the ground swath concept. For near-polar orbits, θ_f intersects the ground swath twice. Consequently the landing approaches are bidirectional, from a northerly direction for one set of calldowns and from a southerly direction for the other. As i is decreased, the total number of calldowns remains essentially constant at first, then rises sharply to reach a peak at $i = \theta_f + R$ for small and moderate maneuvering rectangles, where R is the half-width of the ground swath. At $i = \theta_f + R$ the two ground swath intersections of θ_f coalesce into one and the landing approaches become unidirectional, westerly for a space vehicle in a direct orbit, easterly for one in a retrograde orbit. The number of calldowns goes to zero as i decreases to $\theta_f - R$ and remains zero for $i < \theta_f - R$ (no intersection of θ_f with ground swath). For the largest maneuvering rectangle, $R_{lat} = \pm 2400$ naut miles; hence $R > \theta_f$ and the calldowns increase monotonically with decreasing i until there is a calldown on every revolution for an equatorial orbit when θ_f is wholly within the ground swath. Small irregularities in the calldown curves are due to the coarse subdivision of data points and the variation of τ and Ω with i . The maximum delay time curve is not the inverse of the calldown curve, because for moderate and large maneuvering rectangles the calldown revolutions are concentrated in one or two daily periods

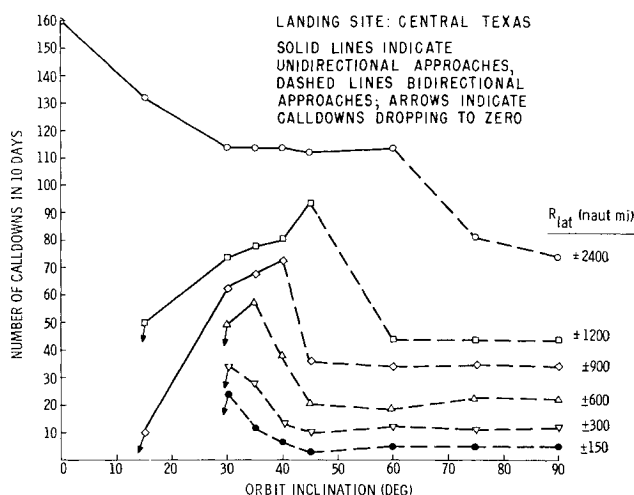


Fig. 1 Number of calldowns to central Texas.

when the landing site is within the ground swath. There is a critical value of R_{lat} between ± 300 and ± 600 naut miles for this space-station mission. Below this value, daily calldowns cannot be guaranteed for all $i > \theta_f$. The maximum delay time curves for maneuvering rectangles that are smaller than critical exhibit an irregular decrease with i which can be explained as follows. Denote the longitude of entry and exit from the ground swath at θ_f by λ_1 and λ_2 , respectively. The coverage longitude, defined as the sum of $\Delta\lambda = \lambda_2 - \lambda_1$ for each ground swath intersection, increases as i decreases from 90° to $\theta_f + R$. Irregularities appear in the maximum delay time curves because variables in addition to the ground swath width become significant. One such variable is the daily shift between space vehicle ground tracks, $d = (360 - K\Delta)$, where Δ is the longitude difference between successive ground tracks and K the closest integer number of revolutions per sidereal day. The other variable, applicable to bidirectional

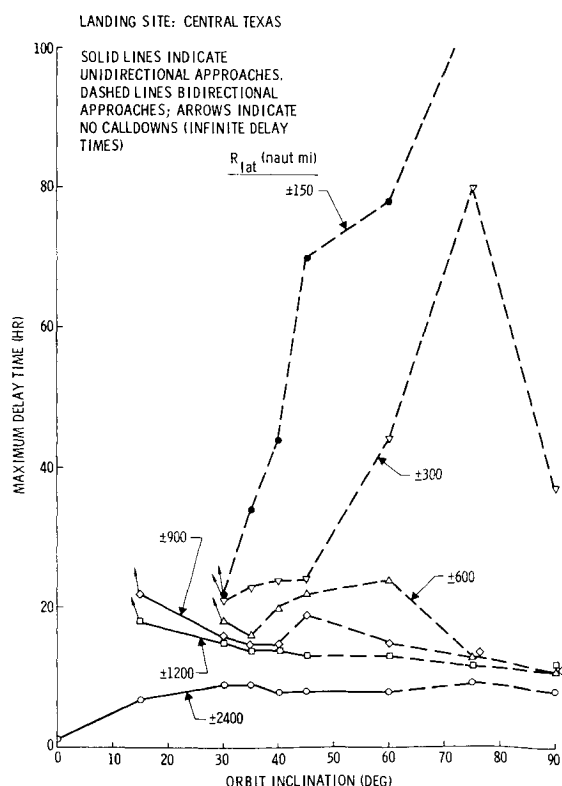


Fig. 2 Maximum delay time for central Texas landings.

approaches only, is the longitudinal spread between the two crossings of θ_f by the vehicle ground track. Both are functions of i and initial altitude. Hence, for small maneuvering rectangles, these orbital parameters should be chosen carefully in order to obtain the lowest maximum delay times.

References

- ¹ Rosamond, D. L., "Satellite recovery techniques for optimization of touchdown accuracy," *J. Aerospace Sci.* **28**, 237-243 (1961).
- ² Jensen, J., Townsend, G. E., Kork, J., and Kraft, J. D., *Design Guide for Orbital Flight* (McGraw-Hill Book Co., Inc., New York, 1962), Chap. IX.
- ³ "Orbital flight handbook," ER 12684, Martin Company, Space Systems Div., Baltimore, Md., Chap. VIII (1963); also NASA SP-33.
- ⁴ Lee, V. A., "Atmosphere-oblateness correction factor for circular satellite orbits," *ARS J.* **32**, 102, 103 (1962).
- ⁵ *U. S. Standard Atmosphere, 1962* (U. S. Government Printing Office, Washington, D. C., 1962).
- ⁶ Kalil, F. and Martikan, F., "Derivation of nodal period of an earth satellite and comparisons of several first-order secular oblateness results," *AIAA J.* **1**, 2041-2046 (1963).

Attitude Sensor for Vehicle Orientation in Space Flight

DAVID W. SWAIN* AND WILLARD H. BENNETT†
*North Carolina State of the University of North
 Carolina at Raleigh, Raleigh, N. C.*

ONE of the most vitally essential operations in manned space flight has been the precise alignment of the vehicle with respect to the orbit and the earth before igniting the retrorockets, and later, the precise realignment of the vehicle before re-entry into the earth's atmosphere. The only instrument system that has been available for these alignments relies upon sensitive precision gyroscopes combined with electronic and timing equipment for calculating the required alignment of the gyroscopes relative to the vehicle. However, in long, sustained flights, any gyroscope has a finite amount of drift that cannot be eliminated. Therefore, it is desirable to have a backup system that operates on an entirely different principle.

An attitude sensing system based on two pairs of ion probes has been developed and tested at North Carolina State in work that has been performed jointly with the Aerospace Division of The Boeing Company in Seattle. At altitudes above 300 kft, the earth's atmosphere is so rarefied that pressure gages cannot measure its density, but the density of the ionized material is more than sufficient to operate the attitude sensor reliably. By comparing the ion currents to the probes, the instrument directly measures the angle between the axis of the vehicle and the direction of motion without any need to know what the previous motion of the vehicle has been or should have been. Since it has no moving parts and has very simple electronics, the durability of this attitude sensor can be expected to be even higher than that of any inertial guidance system.

The two probes of each pair are mounted at an angle relative to each other (Fig. 1). If the probes are moving through an ionized medium, the number of ions that enter each probe will depend on the angle that the probe axis makes with the direction of motion. In a simplified theory, where we assume that the ions have negligible thermal speed

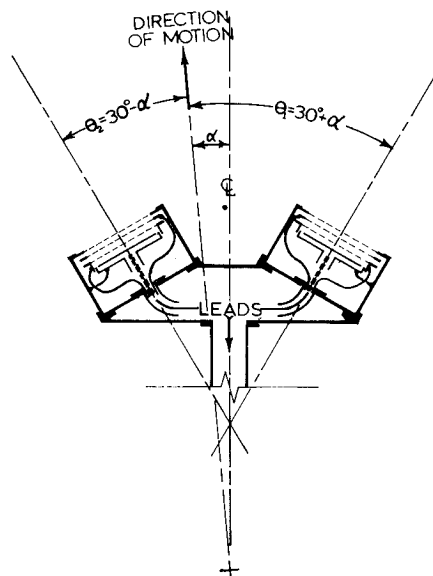


Fig. 1 Angles between velocity vector and ion probes in an attitude sensor.

when compared to the vehicle velocity u , the current i that will reach the collector in one of the probes is

$$i = neuA \cos \theta$$

where n = ion density, e = ion charge (assumed to be +1 electron charge), A = probe area, and θ = angle between the direction of motion and the normal to the grids in that probe.

In the figure, $\theta_1 = 30^\circ - \alpha$ and $\theta_2 = 30^\circ + \alpha$ so the ratio of the currents i_1 and i_2 picked up by probes one and two will be

$$R = i_1/i_2 = \cos(30^\circ - \alpha)/\cos(30^\circ + \alpha)$$

A simple method for finding R electronically is to feed the current from each of the probes into a logarithmic amplifier, so that $V_1 = K \log i_1$, and $V_2 = K \log i_2$, where V_1 and V_2 are the voltage outputs from the two amplifiers. Then the difference between the voltages is:

$$V_1 - V_2 = K[\log i_1 - \log i_2] = K \log(i_1/i_2) = K \log R$$

This voltage difference can be amplified by a transistorized difference amplifier and used to drive a display meter. Using this method, an indication of orientation to $\pm 2^\circ$ accuracy has been obtained by using simple electronics already developed.

An attitude sensor using ion probes that are mostly hollow would, of course, allow air to pass through, and hence, when used on a re-entering vehicle, should operate properly down to lower altitudes than would the above solid-plate type of probes. This kind of ion probe (Fig. 2) consists of a cylindrical outer shell, six control grids made of 0.001-in. knitted tungsten wire, a longitudinal diaphragm running part of the way down the cylinder, and two metal half cylinders inside the shell. The insulation shown may be either Kel-F or Teflon. All elements except grids one and six are insulated from the probe shell. These two grids are grounded to the shell to prevent any electric fields due to potentials inside the probe from extending into the medium outside the probe volume. Thus, the potentials inside the probe do not affect the motion of the charged particles around the probe.

The second grid is the ion-retarding grid. It may be used in one of two different ways, depending on the type of electronic instrumentation used. If a d.c. amplifier is used to read the ion current passing into the probe, the retarding grid is kept at 0 v allowing a steady ion current to flow. If an a.c. amplifier is used, the grid may be commutated be-

Received June 15, 1964; revision received August 31, 1964.

* Department of Physics.

† Burlington Professor of Physics.